Evidence for the extraterrestrial origin of a natural quasicrystal

Luca Bindi[a,b], John M. Eiler[c], Yunbin Guan[c], Lincoln S. Hollister[d], Glenn MacPherson[e], Paul J. Steinhardt[f,g,1], and Nan Yao[h]

[a]Museo di Storia Naturale, Sezione di Mineralogia, Università degli Studi di Firenze, Via La Pira 4, I-50121 Florence, Italy; [b]Dipartimento di Scienze della Terra, Università di Firenze, Via La Pira 4, I-50121 Florence, Italy; [c]Division of Geological and Planetary Sciences, California Institute of Technology, Pasadena, CA 91125; [d]Department of Geosciences, Princeton University, Guyot Hall, Princeton, NJ 08544; [e]Department of Mineral Sciences, National Museum of Natural History, Smithsonian Institution, Washington, DC 20013; [f]Princeton Center for Theoretical Science, Princeton University, Princeton, NJ 08544; [g]Department of Physics, Princeton University, Jadwin Hall, Princeton, NJ 08544; and [h]Princeton Institute for the Science and Technology of Materials, Princeton University, Princeton, NJ 08544

We present evidence that a rock sample found in the Koryak Mountains in Russia and containing icosahedrite, an icosahedral quasicrystalline phase with composition $Al_{63}Cu_{24}Fe_{13}$, is part of a meteorite, likely formed in the early solar system about 4.5 Gya. The quasicrystal grains are intergrown with diopside, forsterite, stishovite, and additional metallic phases [khatyrkite ($CuAl_2$), cupalite (CuAl), and β-phase (AlCuFe)]. This assemblage, in turn, is enclosed in a white rind consisting of diopside, hedenbergite, spinel ($MgAl_2O_4$), nepheline, and forsterite. Particularly notable is a grain of stishovite (from the interior), a tetragonal polymorph of silica that only occurs at ultrahigh pressures (≥ 10 Gpa), that contains an inclusion of quasicrystal. An extraterrestrial origin is inferred from secondary ion mass spectrometry $^{18}O/^{16}O$ and $^{17}O/^{16}O$ measurements of the pyroxene and olivine intergrown with the metal that show them to have isotopic compositions unlike any terrestrial minerals and instead overlap those of anhydrous phases in carbonaceous chondrite meteorites. The spinel from the white rind has an isotopic composition suggesting that it was part of a calcium-aluminum-rich inclusion similar to those found in CV3 chondrites. The mechanism that produced this exotic assemblage is not yet understood. The assemblage (metallic copper-aluminum alloy) is extremely reduced, and the close association of aluminum (high temperature refractory lithophile) with copper (low temperature chalcophile) is unexpected. Nevertheless, our evidence indicates that quasicrystals can form naturally under astrophysical conditions and remain stable over cosmic timescales, giving unique insights on their existence in nature and stability.

Icosahedrite, a naturally occurring quasicrystal, with composition $Al_{63}Cu_{24}Fe_{13}$ and exhibiting Bragg peak diffraction with icosahedral symmetry, was recently discovered in a rock sample found in the Museo di Storia Naturale of the Università degli Studi di Firenze (catalog number 46407/G), labeled as khatyrkite and identified as coming from the Khatyrka ultramafic zone in the Koryak Mountains in the Chukotka Autonomous Okrug of Far Eastern Russia (1, 2). Investigations over the past year have determined that the sample studied here, with size $0.27 \times 0.30 \times 0.32$ cm, is one of two rocks containing khatyrkite ($CuAl_2$) and cupalite (CuAl) to have been found in a claybed at the Listveno-vyi stream in 1979 by V. V. Kryachko, the other being the holotype sample (3) deposited in the St. Petersburg Mining Institute. The holotype is an aggregate of metallic crystals, approximately 1 mm across, with no sign of surrounding host rock-forming minerals visible on the exterior. The interior has not been examined to date. By contrast, the sample studied here shows a remarkably complex set of assemblages (Fig. 1, Fig. 2), with a core containing quasicrystalline icosahedrite, crystalline metallic phases khatyrkite, cupalite, and β-phase (AlCuFe), diopside (Fig. S1), and forsterite (Fig. S2), as well as minute amounts of stishovite; and a white outer rind that contains very fine grained diopside, olivine, nepheline, hedenbergite, and spinel ($MgAl_2O_4$) (Fig. S3). Our grain and the holotype are the only two samples containing khatyrkite and cupalite to have been discovered anywhere to date.

The rock sample was first identified for study as a result of a decade-long systematic search for a natural quasicrystal (4). Quasicrystals are solids whose atomic arrangement exhibits quasiperiodic rather than periodic translational order and rotational symmetries that are impossible for ordinary crystals (5) such as fivefold symmetry in two-dimensions and icosahedral symmetry in three-dimensions. Until recently, the only known examples were synthetic materials produced by melting precise ratios of selected elemental components and quenching under controlled conditions (6–8). The search consisted of applying a set of metrics for recognizing quasicrystals to a database of powder diffraction data (4) and examining minerals outside the database with elemental compositions related to those of known synthetic quasicrystals.

The sample studied here is the only example to emerge from the search to date with a verified quasicrystalline phase, as evidenced by single crystal X-ray and transmission electron microscopy (TEM) diffraction patterns (1). The measured composition of the icosahedrite grains, $Al_{63}Cu_{24}Fe_{13}$, agrees with the ideal stoichiometry of a known quasicrystal synthesized in the laboratory (9). The olivine grains coexisting with this natural quasicrystal are near end-member forsterite [for most grains, the atomic Mg/(Fe + Mg) is in the range 94–99%] and the pyroxene grains are near end-member diopside [$CaMgSi_2O_6$, with atomic Mg/(Fe + Mg) generally 97–99%]. The Fe contents of these grains are too low to state with confidence whether they are in cation-exchange equilibrium at any plausible temperature, but their similarity in Fe content permits the interpretation that olivine and pyroxene in this sample formed together or in geochemically similar environments. Evidence of zoning in P, Cr, and Ni was found in some of the forsterite grains (Fig. S4).

Although Razin et al. (3) describe the khatyrkite holotype sample as being found in clay associated with weathered serpentinite, no evidence or argument supporting a natural origin, terrestrial or extraterrestrial, is presented. In our study, serious consideration was given to numerous theories for how the sample studied here may have originated, particularly the possibility that the rock (because of the Al alloy) is terrestrial or the result of anthropogenic activity (1). Although there is not yet a complete understanding of how the sample formed with all of the observed features, we report in this paper a series of investigations that supersede earlier results and clearly point to an extraterrestrial
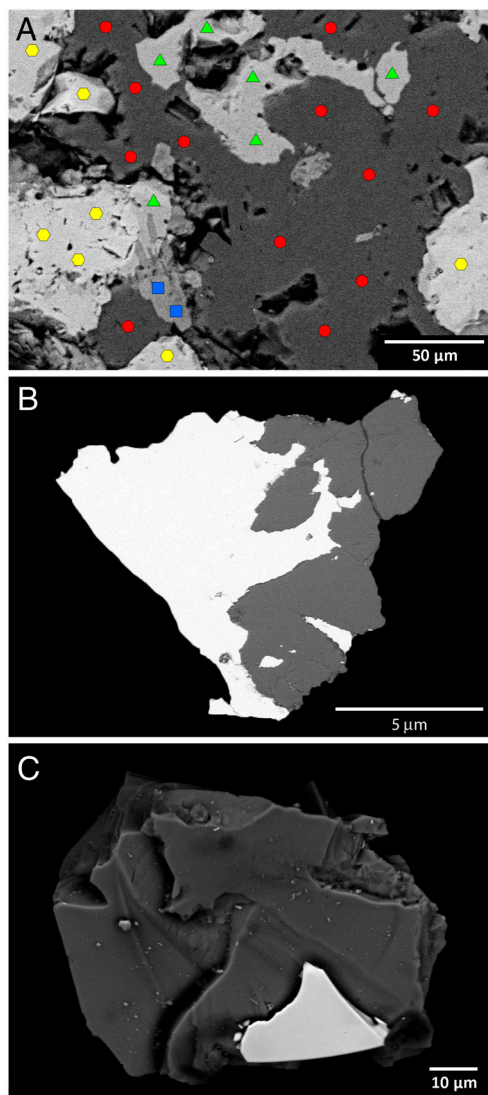
APPLIED PHYSICAL SCIENCES

Fig. 1. (*A*) Backscattered electron image from a thin polished slice of the sample showing the complex intergrowth of metallic and silicate phases. A microprobe analysis was made at each location marked with a symbol (Tables S1–S4): red circles (olivine); blue squares (clinopyroxene); green triangles (khatyrkite); and yellow hexagons (cupalite). (*B*) Micrograin showing an interface between icosahedrite (left, white) and clinopyroxene (right, gray). X-ray element and WDS scans (Fig. S1, Tables S5–S8) show that the icosahedrite composition is $Al_{63}Cu_{24}Fe_{13}$ and clinopyroxene is close to pure $CaMgSi_2O_6$; the scans also show that both phases are extremely homogeneous, with no indication of reaction at the interface. (Reprinted from ref. 2 with permission from Mineralogical Society of America.) (*C*) Micrograin showing an interface between icosahedrite (bottom right, white) and olivine (upper left, gray). X-ray element and WDS scans (Fig. S2, Tables S5–S8) show that the icosahedrite composition is $Al_{63}Cu_{24}Fe_{13}$ and olivine is close to pure Mg_2SiO_4.

origin, from which it is reasonable to infer that the holotype sample is extraterrestrial as well.

Results

An unexpected and critical clue in determining the origin of our sample was the discovery of a 50-nm sized grain of stishovite (Fig. 2*A*), a tetragonal polymorph of silica with $a = 4.2$ Å and $c = 2.7$ Å (identified through TEM; *Inset* and Fig. S5). Stishovite forms at high pressures (e.g., at shock pressures ≥10 GPa and temperatures ≥1,500 K). Its presence strongly points to formation in an extreme environment, as might occur in a hypervelocity impact or in the deep mantle. This stishovite contains inclusions
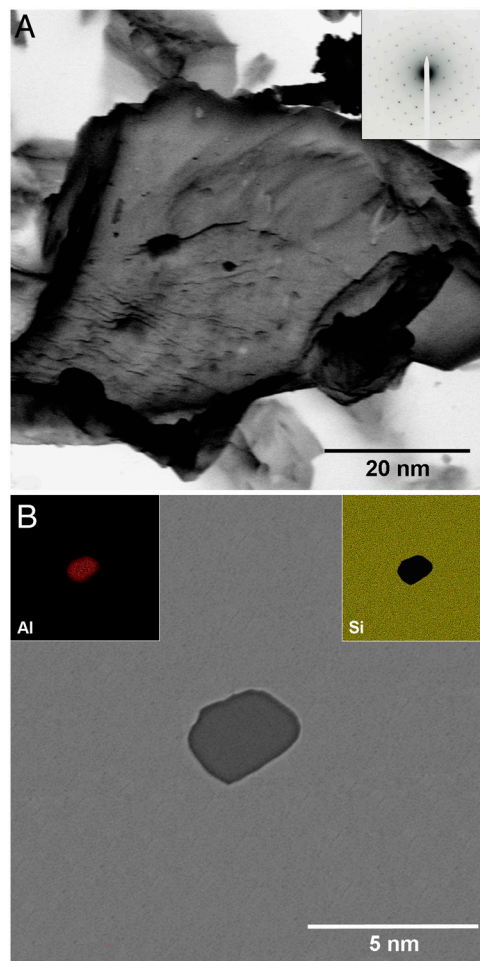
Fig. 2. (*A*) A 50-nm sized grain of stishovite, a tetragonal polymorph of SiO_2, and one of a series of TEM diffraction patterns (*Inset*) taken at different angles that establish the tetragonal symmetry and lattice parameters $a = 4.2$ Å and $c = 2.7$ Å (see also Fig. S5). (*B*) A 5 nm inclusion of icosahedrite $Al_{63}Cu_{24}Fe_{13}$ in the stishovite grain. *Insets* show the Al X-ray element scan (see Fig. S6 for similar Fe and Cu scans), indicating the icosahedrite inclusion, and an Si X-ray element scan indicating the stishovite (see Fig. S6 for similar O scan).

of quasicrystal (Fig. 2*B*, Fig. S6), an indication that the quasicrystal formed before or during an extremely high pressure event.

Clearly, one of the possible implications of the stishovite is a connection with meteorites, which commonly contain products of shock metamorphism. This observation thus motivated an ion probe investigation of the oxygen isotopic composition to determine whether the origin of the sample is terrestrial or extraterrestrial, based on previous evidence for the distinctive differences in oxygen isotope composition between the earth and meteorites (10). Unmetamorphosed and nonaqueously altered carbonaceous chondrites commonly contain minerals that differ markedly in oxygen isotope composition from terrestrial materials because they condensed from or underwent isotopic exchange with nebular gas early in solar system history. These minerals have distinctive ratios of $^{18}O/^{16}O$ and $^{17}O/^{16}O$ compared to the equivalent terrestrial minerals. Fig. 3 is a standard 3-isotope plot showing the measured ratios in various silicate and oxide minerals found in our sample. Terrestrial rocks and water fall on a line of slope approximately 0.5 [the terrestrial fractionation line (TF)] as shown in Fig. S7. Anhydrous minerals from carbonaceous chondrite meteorites [principally minerals in chondrules and calcium-aluminum-rich inclusions (CAIs)] fall on a line of slope approximately 0.94 that extends to very ^{16}O-rich compositions in the case
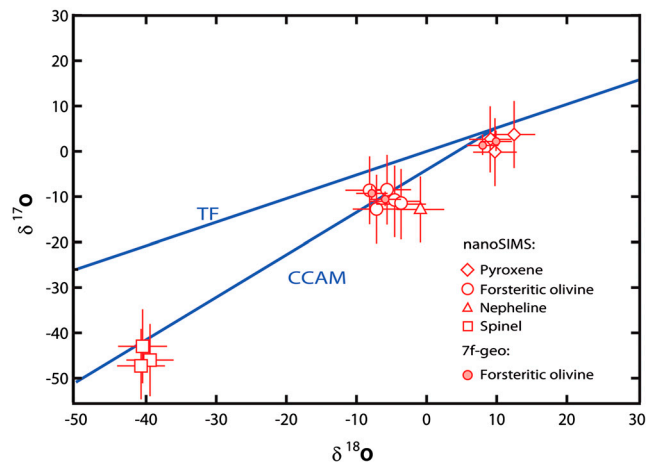
Fig. 3. A plot of oxygen three-isotope composition as suggested by Clayton et al. (10) to discriminate terrestrial and extraterrestrial minerals, containing data for four minerals (pyroxene, nepheline, olivine, and spinel) in the meteorite studied here. The data are compared to concurrent analyses of terrestrial (Burma spinel, San Carlos olivine) and extraterrestrial (Eagle Station olivine) standards in Fig. S7. All data are ion probe measurements made with either the Cameca NanoSIMS (large error bars) or the Cameca img-7f geo (small error bars). The error bars are 2σ. The plotted compositional indices, $\delta^{18}O_{VSMOW}$ and $\delta^{17}O_{VSMOW}$, are the difference in $^{18}O/^{16}O$ and $^{17}O/^{16}O$ ratios, respectively, compared to the ratios in VSMOW, expressed in parts per million. Terrestrial minerals fall along the upper gently sloping line (TF); the oxygen isotope compositions measured for our sample lie along the line corresponding to anhydrous minerals in the CO or CV carbonaceous chondrites (the CCAM).

of CAIs. This line is referred to as the carbonaceous chondrite anhydrous mineral (CCAM) line. Our samples mostly disperse along the CCAM line, and clearly are resolved from the TF line. Spinel, which was only found in grains extracted from the exterior rind of the sample, plots down in the range of CAI spinel, and the only other known solar system materials that plot near such compositions other than CAIs are the solar wind (11) and some types of forsterite-rich meteoritic material, e.g., amoeboid olivine aggregates (12). Therefore the silicates and oxides in our rock sample are indisputably extraterrestrial. The precise relationship of silicate and oxide minerals in our samples to those in relatively well-understood classes of meteorites is ambiguous: The presence of ^{16}O-rich spinel, dominant olivine composition near $\delta^{17}O_{VSMOW} = -10$ and $\delta^{18}O_{VSMOW} \sim -5‰$ (where VSMOW is Vienna standard mean ocean water), and somewhat higher values for nepheline all resemble constituents of CAIs from CV3 and CO3 carbonaceous chondrites. However, the relatively high $\delta^{17}O$ and $\delta^{18}O$ values for clinopyroxene and one olivine grain (from the exterior rind) are more consistent with the isotopic composition of meteorite matrix grains. In any case, the great diversity of oxygen isotope compositions for the phases in our sample precludes any wholesale thermal equilibration after accretion, as would have occurred during partial melting or intense thermal metamorphism. Again, an unequilibrated body such as a carbonaceous chondrite is indicated.

To gain further insight into the origins of the most abundant silicate minerals in the sample we have examined, we used secondary ion mass spectrometry (SIMS) techniques to measure the abundances of rare earth elements in clinopyroxene and olivine (Fig. 4). Clinopyroxenes are characterized by approximately chondritic abundances, light-rare earth depleted rare earth element (REE) patterns and a pronounced negative Eu anomaly. Olivines are characterized by lower overall REE abundances, more extreme light-rare earth depletions, weak Eu anomalies, and, for one grain, a peculiar depletion in Ho and Er compared to adjacent heavy REEs. Although REE profiles for olivine and clinopyroxene from the sample have certain features in common,
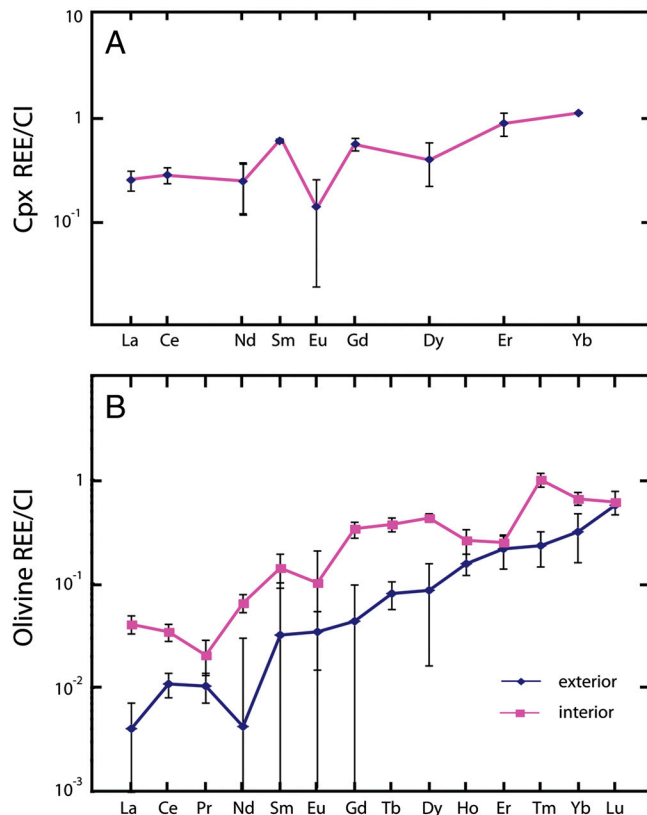

Fig. 4. REE distribution in clinopyroxene (A) and olivine (B). The values have been normalized to the CI chondrite abundances (13).

these minerals cannot be in equilibrium with one another at high (i.e., magmatic or thermal-metamorphic) temperatures. Most obviously, the olivines are diverse in their REE chemistry. Furthermore, REE abundances in olivine are generally greater than those predicted for equilibrium with coexisting clinopyroxene at magmatic temperatures. (These features also differ from those observed in terrestrial ultramafic rocks.)

To search for the former presence of the short-lived extinct radionuclide ^{26}Al at the time of quasicrystal formation, the concentration of the decay product ^{26}Mg in the natural quasicrystal was analyzed with SIMS. Despite extremely high Al/Mg ratios, no detectable radiogenic ^{26}Mg excesses were found in the quasicrystal, implying either that the quasicrystal never contained live ^{26}Al, or that it formed more than three million years later than most CAIs, or that its Mg isotopic composition reequilibrated with coexisting Mg-rich phases after the decay of ^{26}Al.

Discussion

The quasicrystalline phase found in the sample has the same structure and stoichiometry as the first sample of icosahedral $Al_{63}Cu_{24}Fe_{13}$ synthesized and characterized in the laboratory in 1987 (9). Our results push the age of the oldest known example of this phase back to *ca.* 4.5 Gya, the age of all known unequilibrated chondrites. The laboratory samples were prepared under controlled conditions: casting from the melt in an argon atmosphere; solidifying under vacuum at a cooling rate of 1 °C/ min until room temperature; then annealing for 10 d at 825 °C (8, 14). The stability of the phase was examined in a series of studies (8). The range of stable compositions of the quasicrystal phase as a function of temperature narrows as the temperature decreases down to 550 °C, below which isothermal sections are difficult to obtain because of prohibitively long equilibration times (8). At 550 °C there remains a small stability zone centered around the

APPLIED PHYSICAL SCIENCES

stoichiometry measured in our sample (to within measurement uncertainties).

The occurrence of a quasicrystal phase in a meteorite demonstrates that a quasicrystal phase can form naturally within a complex, inhomogeneous medium. The one we describe formed under astrophysical conditions; whether one can form in the course of planetary evolution remains to be determined. From the perspective of condensed matter physics our observations lend support to the original suggestion (5) that quasicrystals can be as stable as other forms of naturally occurring solid matter. The finding of natural quasicrystal enclosed within stishovite indicates either that the quasicrystal formed at high pressure (>7 GPa) or at least remained stable during a later high-P event. Laboratory studies of $Al_{63.5}Cu_{23}Fe_{12.5}$ in diamond-anvil cells (15, 16) at high pressures up to 35 GPa have not shown evidence of a phase transformation, but there have not yet been systematic studies of the phase diagram of quasicrystals at high pressure.

One of the many puzzles presented by our sample is the presence of metallic aluminum, which even in alloys requires highly reducing conditions to form. Metallic aluminum has never been detected even as a trace component in metal within enstatite chondrites and achondrites (aubrites), yet those latter metals do contain significant metallic silicon. It was therefore surprising at first to find in our sample that no metallic silicon existed at the contacts between metal grains and silicates (Fig. 1, Fig. 2). Accordingly, equilibrium thermodynamic calculations, adapting a general method outlined by Essene and Fisher (17) for the study of iron-silicon in a fulgurite, were made to determine the oxygen fugacity required to stabilize khatyrkite (the most extreme case) and cupalite. As these phases are largely iron free (Tables S1–S4), the calculations were simplified relative to what would be required for the icosahedrite itself (Tables S5–S8. Thermodynamic data were taken from Robie et al. (18) and, for activity coefficients in binary Al-Cu melts, from Hultgren et al. (19). The results (Fig. 5) confirm that extreme reducing conditions are required; however, the requisite fO_2 for the khatyrkite curve lies somewhat above the Si-SiO$_2$ buffer curve. This finding resolves the apparent anomaly of finding no metallic silicon at the metal-silicate interfaces. In fact, the fO_2 for khatyrkite is close to the estimated oxygen fugacity of the early solar nebula in the region where CAIs formed (20). Given the association of the metal with CAI phases (especially spinel) in our sample, a nebular origin could provide the necessary conditions to stabilize the metallic alloys. What it does not explain, however, is the association of
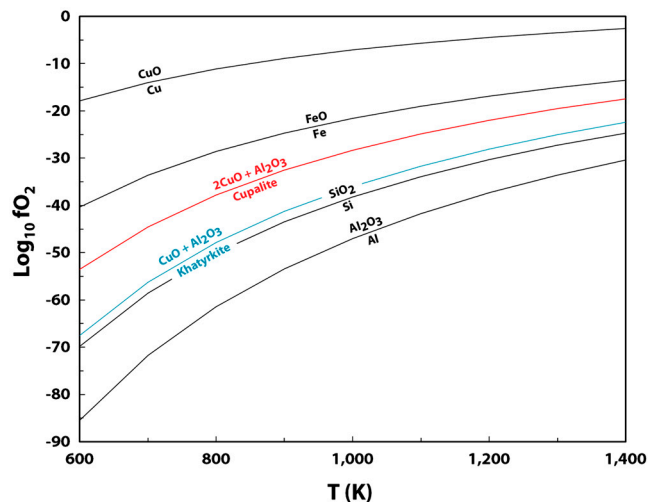
aluminum with copper in the first place. In the context of equilibrium nebular condensation, aluminum is lithophile and condenses at very high temperatures in phases such as aluminates, gehlenite ($Ca_2Al_2SiO_7$), and anorthite ($CaAl_2Si_2O_8$). Copper, on the other hand, is chalcophile (associated with sulfur) and condenses at much lower temperatures than aluminum. The two elements are essentially never associated in chondrites, certainly not in CAIs. Their association in our sample remains an unsolved enigma.

If alloys examined here formed in association with CAIs, as the presence of ^{16}O-rich spinel seems to indicate, they formed at least three million years later than did common CAIs, based on the absence of detectable excess (radiogenic) of ^{26}Mg from the decay of ^{26}Al (i.e., whereas common CAIs have excess ^{26}Mg). Yet if the setting was on the chondrite parent body where copper mobilization might be expected owing to the presence of fluids, the expected fO_2 in such circumstances would be far too high to stabilize metallic copper-aluminum alloys. A conceivable resolution, we speculate, is that a hypervelocity impact on the parent body produced the reducing conditions and that our sample comes from a portion of such a body that had undergone fluid-hosted Cu enrichment prior to shock metamorphism. This speculation may also account for the minute amount of stishovite, which normally does not occur with forsterite and nepheline. This and other speculations are the subject of continuing investigation.

What is clear, however, is that this meteoritic fragment is not ordinary. Resolving the remarkable puzzles posed by this sample will not only further clarify the origin of the quasicrystal phase but also shed light on previously unobserved early solar system processes. Fitting all these clues together in a consistent theory of formation and evolution of the meteorite is the subject of an ongoing investigation.

Experimental Methods

The sample studied here (Mineral Collections of the Museo di Storia Naturale of the Università degli Studi di Firenze, catalog number 46407/G) was found to consist of a core with metallic phases intergrown with forsteritic olivine, diopsidic clinopyroxene, and a minute amount (50-nm sized grain) of stishovite, and a white external rind consisting primarily of silicates (forsteritic olivine, diopsidic clinopyroxene, hedenbergite, nepheline, and sodalite), oxides (spinel), and small amounts of metallic phases. The exterior rind was removed, and the core was sliced into thin sections (e.g., Fig. 1A), which were carefully studied with an electron microprobe. When the chemical analyses obtained at the microprobe showed similarities with those of known quasicrystals, individual samples of each metallic phase with its surrounding material were extracted to perform X-ray diffraction studies. Because the process destroyed the integrity of the thin sections, the remaining studies in this paper are obtained from exhaustive examination of the grains extracted from both the interior and exterior of the sample.

The grain with quasicrystal and diopside (Fig. 1B, grain used for REE studies), a large olivine grain used in the O-isotope studies, and the tiny stishovite grain with quasicrystal inclusion (Fig. 2), were all in the same interior sample containing predominantly quasicrystal. As shown in the figures, examples of olivine and clinopyroxene in direct contact with quasicrystal have been observed. Spinel, whose O-isotope composition most strongly indicates CAI, was only found in the exterior white rind material; direct contact with quasicrystal has not been observed.

SEM. The instrument used was a Zeiss-EVO MA15 Scanning Electron Microscope coupled with an Oxford INCA250 energy-dispersive spectrometer, operating at 25 kV accelerating potential, 500 pA probe current, 2,500 cps as average count rate on the whole spectrum, and a counting time of 500 s. Samples were

Fig. 5. Log$_{10}$ fO_2 vs. T (K) equilibriums curves for several metal—metal oxide pairs and for cupalite and khatyrkite. The latter alloys require highly reducing conditions to form relative to their stoichiometric oxides, but not so reducing as for pure Al or Si.

sputter-coated with 30-nm thick carbon film. X-ray maps were collected with acquisition times of 10 ms per pixel.

Electron Microprobe. *X-ray intensity maps.* $K\alpha$ X-ray intensity maps of Al, Cu, Fe, Ca, Cr, Mg, Na, and Si for silicates (olivine and clinopyroxene) and metal alloys (khatyrkite, cupalite, and icosahedrite) were obtained using a JEOL JXA-8600 electron microprobe operating at an accelerating voltage of 15 kV, beam current of 300 nA, and a beam diameter of 1 μm. Beam current variations during map acquisition were $\leq$4 nA. Acquisition times of 180 ms were used for the map of Cu, Al, Ca, Mg, and Si (acquired at the same time), whereas acquisition times of 300 ms were used for Fe, Cr, and Na maps (acquired at the same time). Maps only show X-ray intensity (i.e., neither calibrations nor background corrections were applied).

Wavelength dispersive spectroscopy (WDS) spots. Metal alloys (khatyrkite, cupalite, and icosahedrite). Major and minor elements were determined at 15 kV accelerating voltage and 20 nA beam current (and a 1 μm beam diameter), with variable counting times: 30 s were used for Al, Cu, and Fe, and 100 s for the minor elements Mg, Si, Cr, P, Co, Ni, Cl, Ca, Zn, and S. Replicate analyses of synthetic $Al_{63}Fe_{24}Cu_{13}$ quasicrystal (8) were used to check accuracy and precision. The standards used were: metal-Al (Al), metal-Cu (Cu), synthetic FeS (Fe), metal-Co (Co), synthetic ZnS (Zn, S), synthetic Ni_3P (Ni, P), synthetic $CaCl_2$ (Ca, Cl), metal-Mg (Mg), metal-Si (Si), and metal-Cr (Cr).

Silicates (olivine and clinopyroxene). Major and minor elements were determined at 15 kV accelerating voltage and 40 nA beam current (and a 1 μm beam diameter), with variable counting times: 30 s were used for Ca, Mg, and Si, and 100 s for the minor elements Fe, Cr, Na, Ti, Al, Mn, P, Cu, Co, and Ni. Matrix correction was performed using the Bence and Albee program (21) modified by Albee and Ray (22). Replicate analyses of augite USNM 122142 were used to check accuracy and precision. The standards used were: diopside (Ca), forsterite (Mg), bustamite (Mn), ilmenite (Fe), sphaerocobaltite (Co), bunsenite (Ni), albite (Na, Al, Si), eskolaite (Cr), rutile (Ti), cuprite (Cu), and apatite (P).

TEM. Studies were done using a JEOL JEM-2010, an accelerating voltage of 200 kV, an ultrahigh resolution pole piece, and a point-to-point resolution close to 1.9 Å (the electron probe can be focused down to 100 Å in diameter). The microscope is equipped with a semi-STEM system and an energy-dispersive spectrometer (EDS) (ISIS Oxford, superthin window). A small amount of icosahedrite (the same specimen used for the X-ray diffraction study) was placed on a Cu mesh grid (300 mesh, 3 mm in diameter) that had been previously covered by a thin carbon layer (support film). The powdered grid was further coated by carbon.

Selected area diffraction patterns were collected on different orientations for stishovite. In particular, we collected electron diffraction patterns corresponding to the [001], [010], and [0–11], zone axes. X-maps for Si, O, Cu, Al, and Fe were collected with 180 s as acquisition time. The same elements (Si, O, Cu, Al, and Fe) were quantified by using theoretical k-factors in the INCA spectrum analyzer software. Care was taken to make results internally consistent. The electron dose was maintained as far as possible constant from place to place by always using the same spot size, acquisition time, and mean counting rate. TEM–EDS analyses collected on the icosahedrite encased in stishovite gave the following mean values (in wt % of elements and with the standard deviations in parentheses): Al 43.4(2.5), Cu 38.5(1.9), and Fe 18.1(1.3). These values are in good agreement with those obtained for icosahedrite with the electron microprobe.

SIMS and NanoSIMS—Oxygen Isotope Data. Oxygen isotopic compositions of large olivine grains were made using either the

Cameca NanoSIMS 50L or the Cameca ims-7f geo ion microprobe (open and shaded symbols in Fig. 3, respectively). Note that measurements made with the ims-7f geo were made with a relatively large ($\sim$15 μm), intense (0.2 nA) primary ion beam and resulted in relatively precise measurements ($\sim \pm$2–2.5‰ for both ^{17}O and ^{18}O, 2σ), whereas measurements made with the NanoSIMS 50 L were made with a relatively small (3×3 μm), weak ($\sim$30 pA) primary ion beam and resulted in less precise measurements ($\sim \pm$4‰ for ^{17}O and $\sim \pm$8‰ for ^{18}O, 2σ). This combination of instruments and methods permitted us to make a relatively confident analysis of the two large olivine grains available for this study, as well as a large number of less precise analyses of the more numerous and diverse small grains. Uncertainties on individual analyses include analytical errors and statistical variation on repeated analyses of the standards. Standards used for this analysis are San Carlos olivine, Eagle Station olivine, and Burma spinel. On the ims-7f geo, secondary ions were collected by peak-jumping into either a Faraday cup ($^{16}O^-$) or electron multiplier ($^{17}O^-$ and $^{18}O^-$) at a mass resolving power of approximately 6,500, easily resolving the $^{16}OH^-$ interference on $^{17}O^-$; whereas on the NanoSIMS, all the secondary ion signals were simultaneously collected with EMs on a multicollection system, under high mass resolution conditions that resolve any interferences to the mass peaks of interest.

SIMS—Trace Elements in Olivine. Rare earth and other selected trace elements in olivine were measured using a Cameca ims-7f geo ion microprobe. The analytical methods are similar to those described by Zinner and Crozaz (23). A -13.5 keV O$^-$ primary ion beam of approximately 10 nA was used to sputter positive secondary ions from the surface of the sample. Elemental concentrations were determined by counting, at low mass resolution with 80 eV of energy filtering, the secondary ions of appropriate isotopes and comparing these to the count rate from a reference element of known concentration. Although molecular ions can interfere with the atomic ions used to determine elemental concentrations, complex molecular ions tend to have relatively low energies and, thus, can be effectively eliminated by energy filtering. However, simple molecular ions, such as SiO^+ or (LREE) O^+, cannot be entirely filtered out in this manner. Deconvolution of the secondary ion signals of HREEs was done based on Zinner and Crozaz (23). NBS610 and NBS612 glasses were used as standards to determine the relative sensitivity factors for the elements. Si was used as the reference element for all the measurements.

SIMS—Trace Elements in Clinopyroxene. Rare earth and other trace elements in clinopyroxene were measured using a Cameca ims-4f ion microprobe. The sample was sputtered with a 12.5 kV $^{16}O^-$ primary beam at approximately 9.5 nA intensity. Secondary ions were extracted and focused under an ion-image field of 2 μm. The signals from one isotope of each investigated REE was studied, i.e., ^{139}La, ^{140}Ce, ^{146}Nd, ^{149}Sm, ^{153}Eu, ^{158}Gd, ^{163}Dy, ^{167}Er, and ^{174}Yb. The $^{30}Si^+$ ion signal was selected as the isotope of the reference element (Si) for these matrices. Quantification of ion signals was carried out by means of the empirical approach of relative sensitivity factors that were derived from international clinopyroxene standards: KH1 (Kilbourne Hole) (24) and Kakanui augite (25). Concerning the other trace elements, we measured signals from the following isotopes: ^{45}Sc, ^{47}Ti, ^{51}V, ^{52}Cr, ^{88}Sr, ^{89}Y, and ^{90}Zr. Hf was detected through two isotopes, $^{178}Hf^+$ and $^{180}Hf^+$, to check for the presence of residual interferences. All of these trace elements including REE were detected in the same analytical run. Analytical precision from counting statistics is on the order of 10% at parts per million level. Similar values pertain to accuracy.

SIMS and NanoSIMS—Mg Isotope Data. To search for prepresent short-lived radionuclide ^{26}Al, a natural quasicrystal of approximately 10–15 μm was measured by both the NanoSIMS and the ims-7f geo. Terrestrial standards of AlCu alloys, Mg metal, Burma spinel, and synthetic quasicrystal (8) were used to deduce the sensitivity factor for Al/Mg and to correct the instrumental and intrinsic mass fractionations. Considering its small size, the Mg isotope of the quasicrystal was first measured with the Nano-SIMS. However, large erroneous positive δ^{25}Mg values were obtained from the NanoSIMS measurements, mostly due to the combination of low ^{25}Mg count rates and the contribution of unknown scattering ions at the same mass in the NanoSIMS multicollection system. Reliable Mg isotope results of the quasicrystal were then acquired with the ims-7f geo. Briefly, an approximately 0.1 nA O$^-$ primary beam of -13.5 keV was focused into a <5-μm diameter spot for the analyses. The sample voltage was set to +9 keV and secondary ions were collected with an energy band-pass of approximately 40 eV, an imaged field of approximately 75 μm, and a mass resolving power of approximately 4,000. The masses measured were ^{24}Mg, ^{25}Mg, ^{26}Mg, and ^{27}Al. Excesses of ^{26}Mg($\equiv^{26}$Mg*), corrected for both instrumental and intrinsic mass fractionations, were calculated using a linear law; for the high Al/Mg samples, possible errors in determining radiogenic ^{26}Mg* due to an incorrectly applied mass fractionation correction are negligible.

1. Bindi L, Steinhardt PJ, Yao N, Lu PJ (2009) Natural quasicrystals. *Science* 324:1306–1309.
2. Bindi L, Steinhardt PJ, Yao N, Lu PJ (2011) Icosahedrite, Al$_{63}$Cu$_{24}$Fe$_{13}$, the first natural quasicrystal. *Am Mineral* 96:928–931.
3. Razin LV, Rudashevskij NS, Vyalsov LN (1985) New natural intermetallic compounds of aluminum, copper and zinc—khatyrkite CuAl$_2$, cupalite CuAl and zinc aluminides from hyperbasites of dunite-harzburgite formation. *Zapiski Vses Mineral O-va* 114:90–100.
4. Lu PJ, Deffeyes K, Steinhardt PJ, Yao N (2001) Identifying and indexing icosahedral quasicrystals from powder diffraction patterns. *Phys Rev Lett* 87:275507.
5. Levine D, Steinhardt PJ (1984) Quasicrystals: A new class of ordered structures. *Phys Rev Lett* 53:2477–2480.
6. Shechtman D, Blech I, Gratias D, Cahn J (1984) Metallic phase with long-range orientational order and no translational symmetry. *Phys Rev Lett* 53:1951–1954.
7. Janot C (1984) *Quasicrystals: A Primer* (Oxford University Press, Oxford).
8. Bancel PA (1991) *Quasicrystals: The State of the Art*, eds D DiVincenzo and PJ Steinhardt (World Scientific, Singapore), pp 17–56.
9. Tsai AP, Inoue A, Masumoto T (1987) A stable quasicrystal in Al-Cu-Fe system. *Jpn J Appl Phys* 26:L1505.
10. Clayton RN, Onuma N, Mayeda TK (1976) A classification of meteorites based on oxygen isotopes. *Earth Planet Sci Lett* 30:10–18.
11. McKeegan KD, et al. (2011) The oxygen isotopic composition of the sun inferred from captured solar wind. *Science* 332:1528–1532.
12. Krot AN, McKeegan KD, Leshin LA, MacPherson GJ, Scott ERD (2002) Existence of an ^{16}O-rich gaseous reservoir in the solar nebula. *Science* 295:1051–1054.
13. Anders E, Grevesse N (1989) Abundances of the elements: Meteoritic and solar. *Geochim Cosmochim Acta* 53:197–214.
14. Audier M, Guyot P, Brechet Y (1990) High-temperature stability and faceting of the icosahedral Al-Fe-Cu phase. *Philos Mag* 61:55–62.
15. Sadoc A, et al. (1994) X-ray absorption and diffraction spectroscopy of icosahedral Al-Cu-Fe quasicrystals under high pressure. *Philos Mag* 70:855–866.
16. Gupta AJ, Neelima P, Vijaykumar V, Godwal BK (2004) High pressure Mössbauer studies of stable quasicrystal Al$_{63.5}$Cu$_{24}$Fe$_{12.5}$. *J Non-Cryst Solids* 334–335:243–246.
17. Essene EJ, Fisher DC (1986) Lightning strike fusion: Extreme reduction and metal-silicate liquid immiscibility. *Science* 234:189–193.
18. Robie RA, Hemingway BS, Fisher JR (1979) Thermodynamic Properties of Minerals and Related Substances at 298.15 K and 1 Bar (10^5 Pascals) Pressure and at Higher Temperatures. *US Geological Survey Bulletin*, (US Government Printing Office, Washington, DC), Vol 1452 p 456.
19. Hultgren R, Desai PD, Hawkins DT, Gleiser M, Kelley KK (1973) Selected values of the thermodynamic properties of binary alloys. (American Society for Metals, Metals Park, OH) p 1435.
20. Grossman L, Beckett JR, Fedkin AV, Simon SB, Ciesla FJ (2008) Redox conditions in the solar nebula: Observational, experimental and theoretical constraints. *Oxygen in the Solar System Reviews in Mineralogy and Geochemistry*, eds GJ MacPherson, DW Mittlefehldt, JH Jones, and SB Simon (Mineralogical Society of America, Chantilly, VA), Vol 68, pp 93–140.
21. Bence AE, Albee AL (1968) Empirical correction factors for the electron microanalysis of silicate and oxides. *J Geol* 76:382–403.
22. Albee AL, Ray L (1970) Correction factors for electron probe analysis of silicate, oxides, carbonates, phosphates, and sulfates. *Anal Chem* 42:1408–1414.
23. Zinner E, Crozaz G (1986) A method for the quantitative measurement of rare earth elements in the ion microproibe. *Int J Mass Spectrom Ion Processes* 69:17–38.
24. Irving AJ, Frey FA (1984) Trace element abundances in megacrysts and their host basalts: Constraints on partition coefficients and megacryst genesis. *Geochim Cosmochim Acta* 48:1201–1221.
25. Mason B, Allen RO (1973) Minor and trace elements in augite, hornblende, and pyrope megacrysts from Kakanui, New Zealand. *J Geol Geophys* 16:935–947.